Symmetry decomposition of potentials with channels

1997 J. Phys. A: Math. Gen. 30 533

(http://iopscience.iop.org/0305-4470/30/2/018)

J. Phys. A: Math. Gen. **30** (1997) 533–557. Printed in the UK PII: S0305-4470(97)77810-7

Symmetry decomposition of potentials with channels

N D Whelan

Division de Physique Théorique†, Institut de Physique Nucléaire, 91406 Orsay Cedex, France

Received 13 September 1996

Abstract. We discuss the symmetry decomposition of the average density of states for the two-dimensional potential $V = x^2y^2$ and for its three-dimensional generalization $V = x^2y^2 + y^2z^2 + z^2x^2$. In both problems, the energetically accessible phase space is non-compact due to the existence of infinite channels along the axes. It is known that in two dimensions the phase space volume is infinite in these channels thus yielding non-standard forms for the average density of states. Here we show that the channels also result in the symmetry decomposition having a much stronger effect than in potentials without channels, leading to terms which are essentially leading order. We verify these results numerically and also observe a peculiar numerical effect which we associate with the channels. We additionally show that the next-order corrections are anomalously weak, being at least two powers of $\hbar$ smaller than one would expect. In three dimensions, the volume of phase space is finite and the symmetry decomposition follows more closely that for generic potentials—however, there are still non-generic effects related to some of the group elements.

0. Introduction

The role of chaos in the classical Yang–Mills fields has been examined by several authors, the studies have typically been divided into two régimes. In the first, one studies the full field theory [1] and tries to determine such global measures of chaos as the spectrum of Lyapunov exponents and spatial-temporal correlations. In the second, one studies the homogeneous or zero-dimensional limit of the problem [2] which admits a more microscopic analysis. Following this approach, one is led to consider the three-dimensional potential $V = x^2y^2 + y^2z^2 + z^2x^2$ and its simpler two-dimensional cousin $V = x^2y^2$. The two-dimensional problem has been independently studied as it is an interesting dynamical system in its own right. Until Dahlqvist and Russberg showed otherwise [3], it was commonly believed that the classical motion in this potential was completely chaotic. Although this is not true, it remains one of the most chaotic potential systems known. It also serves as a useful example of intermittency [4, 5]. Far from the origin, the motion is confined within one of four channels within which the problem is adiabatic so that a trajectory behaves in a smooth, regular manner. Upon exiting the channel, the trajectory may undergo a burst of strongly irregular motion before re-entering one of the channels. This form of dynamics, regular behaviour with episodes of irregularity, is called intermittency and is found in various physical systems including the classical helium atom [6] and the hydrogen atom in a strong magnetic field [7]. The first of these is governed by a potential very similar in form to x^2y^2 [8]. The three-dimensional problem shares the properties of strong chaos and intermittency although this has been less extensively studied. Additionally, the two-dimensional problem

† Unité de recherche des Universités de Paris XI et Paris VI associée au CNRS.

0305-4470/97/020533+25$19.50

has been shown to have interesting, non-generic level statistics [9] due to the channels. It has been used as a test-case for quantization based on adiabatic separation [10] and for semiclassical quantization based on the heat kernel [11].

We will be interested in the quantization of these potentials, particularly in their densities of states. As proved by Simon [12] and later analysed in greater detail by Tomsovic [13], the two-dimensional potential has a discrete quantum spectrum in spite of having an energetically accessible phase space of infinite volume. This potential therefore violates the semiclassical relation that the number of quantum energy levels below a given energy is, on average, proportional to the volume of energetically accessible classical phase space. In this paper we discuss a related property of this potential—the manner in which the average density of states decomposes among the various irreducible representations (irreps). Normally, the ratio of the number of states belonging to a given irrep R of dimension d_R is roughly $d_R^2/|G|$ [14, 15], where $|G|$ is the order of the group. There are then small $\bar{h}$ corrections depending on the symmetry properties of the irreps [15–17]. We will show here that for the potentials mentioned above, the symmetry 'corrections' can be anomalously large and in two dimensions are essentially leading order.

The relevant symmetry groups for the two- and three-dimensional potentials are C_{4v} and the extended octahedral group respectively ('extended' because we allow for inversions as well as rotations). These groups have five and 10 conjugacy classes of group elements, respectively, and we need to analyse them all in order to calculate the average density of each irrep. The method for doing this when there are no channels is discussed in [15] for reflection operations and [16] in the context of the permutation group. It is then developed in a more general context in [17]. For some of the classes which appear here, the calculation is a straight-forward application of this theory. For other classes, however, the channel effects make it inapplicable and we use a different analysis based on the adiabatic nature of the Hamiltonian deep in the channels as introduced in [13]. In both two and three-dimensions, each channel calculation involves an analysis of the subgroup which leaves that channel invariant.

In the next section, we review the formalism used in constructing the average density of states from approximations of the heat kernels. The approximations are based on Wigner transforms of the Hamiltonian and of unitary transformations which correspond to the group elements. This formalism will be used in the central region of the potential but will be adapted for application in the channels. In section 2 we apply this to the two-dimensional potential and show that there are very strong effects arising from this decomposition—much stronger than one would expect for a normal bound potential. In section 3, we verify these results numerically and also point out the existence of a subtle numerical effect which is only apparent on doing the symmetry decomposition. In section 4, we show that the higher-order $\bar{h}$ corrections are anomalously weak so that the leading-order results give results which are already very accurate. In section 5 we introduce the three-dimensional generalization and discuss the Wigner transforms corresponding to the various group elements. In section 6 we do the channel analysis of the three-dimensional problem and use this to obtain the final results for all classes. In three dimensions, the channel effects are less dramatic but still introduce modifications to what one expects for a generic potential.

1. Formalism

We will interest ourselves in the smooth average part $\bar{\rho}(E)$ of the density of states, often called the Thomas–Fermi term. There is also an oscillating part $\rho_{\rm osc}(E)$ given by periodic orbits [18] but we will not discuss this in detail so in what follows we suppress the bar

on the smooth functions. The specification of only concerning ourselves with the Thomas–Fermi term in the density of states is made by invoking $\hbar$ expansions rather than expansions involving oscillatory functions of $1/\hbar$. One way to find the Thomas–Fermi density of states is to work with the partition function (often called the heat kernel), which is the Laplace transform of the density of states,

$$Z(\beta) = \mathrm{Tr}(\mathrm{e}^{-\beta\hat{H}}) = \mathcal{L}(\rho(E)). \tag{1.1}$$

In the presence of a symmetry group, each quantum state will belong to one specific irrep of that group so we will consider the heat kernels of each irrep separately,

$$Z_R(\beta) = \mathrm{Tr}(\hat{P}_R \mathrm{e}^{-\beta\hat{H}}). \tag{1.2}$$

$\hat{P}_R$ is the projection operator onto the irrep R and for a discrete group is given by [19]

$$\hat{P}_R = \frac{d_R}{|G|}\sum_g \chi_R^*(g)\hat{U}(g). \tag{1.3}$$

The sum is over the elements of the group, $|G|$ in number, $\chi_R(g)$ is the character of group element g in irrep R, d_R is the-dimension of irrep R and $\hat{U}(g)$ is the unitary operator corresponding to the element g,

$$\langle \boldsymbol{r}|\hat{U}(g)|\psi\rangle = \langle g^{-1}\boldsymbol{r}|\psi\rangle = \psi(g^{-1}\boldsymbol{r}). \tag{1.4}$$

One standard way to proceed is to find the Wigner transform [20] of the operators $\mathrm{e}^{-\beta\hat{H}}$ and $\hat{P}_R$ and integrate them to evaluate the trace. The Wigner transform $A_W(\boldsymbol{q},\boldsymbol{p})$ of a quantum operator $\hat{A}$ is a representation in classical phase space, otherwise known as a symbol, and is defined by

$$A_W(\boldsymbol{q},\boldsymbol{p}) = \int \mathrm{d}\,\boldsymbol{x}\left\langle \boldsymbol{q}+\frac{\boldsymbol{x}}{2}\right|\hat{A}\left|\boldsymbol{q}-\frac{\boldsymbol{x}}{2}\right\rangle \mathrm{e}^{-\mathrm{i}\boldsymbol{p}\cdot\boldsymbol{x}/\hbar}. \tag{1.5}$$

Traces are simply evaluated in this representation since

$$\begin{aligned}\mathrm{Tr}(\hat{A}) &= \frac{1}{(2\pi\hbar)^n}\int \mathrm{d}\boldsymbol{q}\,\mathrm{d}\boldsymbol{p}\,A_W(\boldsymbol{q},\boldsymbol{p})\\ \mathrm{Tr}(\hat{A}\hat{B}) &= \frac{1}{(2\pi\hbar)^n}\int \mathrm{d}\boldsymbol{q}\,\mathrm{d}\boldsymbol{p}\,A_W(\boldsymbol{q},\boldsymbol{p})B_W(\boldsymbol{q},\boldsymbol{p})\end{aligned} \tag{1.6}$$

where n is the-dimension of the system. As we will see below, a naive application of these formulae may diverge in the channels; nevertheless, the formalism can be adapted. We will limit the discussion to Hamiltonians of potential systems in which there is no mixing of momenta and coordinates. For the operator $\mathrm{e}^{-\beta\hat{H}}$ we make use of the relation [20]

$$(\mathrm{e}^{-\beta\hat{H}})_W = \mathrm{e}^{-\beta H_W}\left[1+\hbar^2\left\{-\frac{\beta^2}{8}\nabla^2 V+\frac{\beta^3}{24}\left((\boldsymbol{p}\cdot\boldsymbol{\nabla})^2 V+(\boldsymbol{\nabla}V)^2\right)\right\}+\mathrm{O}(\hbar^4)\right] \tag{1.7}$$

where the higher-order terms in the expansion can be found [21, 15]. (See also [22] for an energy representation of the expansion.) To leading order, it is valid to replace $(\mathrm{e}^{-\beta\hat{H}})_W$ by $\mathrm{e}^{-\beta H_W}$ where the Wigner transform of the quantum Hamiltonian H_W is simply the classical Hamiltonian.

In the evaluation of the Wigner transform of the projection operators (1.3), we need the Wigner transforms of the unitary operators $\hat{U}(g)$. This is discussed in detail in [17]; the results for all possible group elements in two-dimensions are,

$$\begin{aligned}&U(I)_W(\boldsymbol{q},\boldsymbol{p}) = 1\\ &U(\sigma_i)_W(\boldsymbol{q},\boldsymbol{p}) = \pi\hbar\delta(q_i)\delta(p_i)\\ &U(R_\theta)_W(\boldsymbol{q},\boldsymbol{p}) \approx \frac{\pi^2\hbar^2}{\sin^2(\theta/2)}\delta(q_1)\delta(q_2)\delta(p_1)\delta(p_2).\end{aligned} \tag{1.8}$$

The Wigner transform of the identity operator gives unity; the transform of a reflection operator gives the delta functions of the position and momentum corresponding to the symmetry plane; and, the transform of a rotation gives the delta functions evaluated at the symmetry axis. (The third result is exact for $\theta = \pi$, otherwise it has higher-order $\overline{h}$ contributions.) An additional property is that a group element in three or higher-dimensions can be decomposed into a product of reflections and rotations in such a way that its Wigner representation is simply the product of the Wigner representations of the reflections and rotations [17]. This is a special property which arises from the fact that the reflections and rotations are functions of mutually orthogonal coordinates. Using this, we obtain from (1.8) the following relations for the three-dimensional operators

$$\begin{aligned} U(\sigma_1\sigma_2\sigma_3)_W(\boldsymbol{q},\boldsymbol{p}) &= \pi^3\overline{h}^3\delta(\boldsymbol{q})\delta(\boldsymbol{p}) \\ U(\sigma R_\theta)_W(\boldsymbol{q},\boldsymbol{p}) &\approx \frac{\pi^3\overline{h}^3}{\sin^2(\theta/2)}\delta(\boldsymbol{q})\delta(\boldsymbol{p}). \end{aligned} \tag{1.9}$$

The first of these says that the transform of the product of three perpendicular reflections gives delta functions in all coordinates and momenta. The second says that the transform of a reflection through a plane times a rotation about the perpendicular axis gives the same delta functions. In both (1.8) and (1.9), the relative power of $\overline{h}$ equals the co-dimension of the set of points left invariant by the group element. We follow [17] in constructing 'class heat kernels'

$$Z(g;\beta) = \mathrm{Tr}(\hat{U}(g)\mathrm{e}^{-\beta\hat{H}}) \tag{1.10}$$

so that

$$Z_R(\beta) = \frac{d_R}{|G|}\sum_g \chi_R^*(g)Z(g;\beta). \tag{1.11}$$

The functions defined in equation (1.10) are 'class functions'; they do not depend explicitly on the group element g but only on the class to which it belongs.

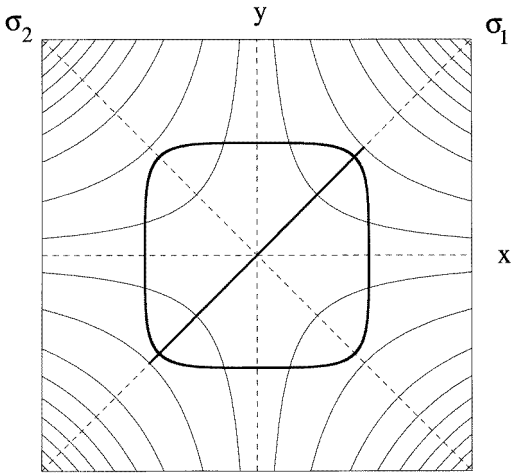

Figure 1. The configuration space of the x^2y^2 potential. The light full curves are constant energy contours at $E = 0.1, 1, 3, 5, \cdots$ and the four broken lines indicate the axes through which the system has a reflection symmetry. The two heavy curves show the two shortest periodic orbits in the system calculated at $E = 1$.

Table 1. Character table of the group C_{4v}.

	I	$\sigma_{x,y}$	$\sigma_{1,2}$	$R_{\pm\pi/2}$	R_π
A_1	1	1	1	1	1
A_2	1	−1	1	−1	1
B_1	1	1	−1	−1	1
B_2	1	−1	−1	1	1
E	2	0	0	0	−2

2. The potential $V = x^2y^2$

The equipotential curves of this potential are shown as the light curves in figure 1. The symmetry group is C_{4v}, the same as that of the square, and consists of eight elements: the identity $\{I\}$; reflections through the channel axes $\{\sigma_x, \sigma_y\}$; reflections through the diagonal axes $\{\sigma_1, \sigma_2\}$; rotations by angle $\pi/2$, $\{R_{\pi/2}, R_{-\pi/2}\}$; and, rotation by angle π, $\{R_\pi\}$. These five sets of elements comprise the five conjugacy classes. It follows that there are five irreps, four are one-dimensional and one is two-dimensional. The character table is given in table 1.

We set out to calculate the five heat kernels corresponding to the five classes. In this section we will only consider the leading-order term of (1.7). The integral corresponding to the identity is then

$$Z(I;\beta) \approx \frac{1}{(2\pi\bar{h})^2}\int \mathrm{d}x\,\mathrm{d}y\,\mathrm{d}p_x\,\mathrm{d}p_y\,\mathrm{e}^{-\beta H} \tag{2.1}$$

where $H = (p_x^2 + p_y^2)/2 + x^2y^2$ is the classical Hamiltonian (and the Wigner transform of the quantum Hamiltonian). This integral is extensively discussed in [13] where it is shown that it has a logarithmic divergence; we return to this point below. According to equations (1.6) and (1.8), the integral corresponding to σ_y is given by

$$Z(\sigma_y;\beta) \approx \frac{1}{(2\pi\bar{h})^2}\int \mathrm{d}x\,\mathrm{d}y\,\mathrm{d}p_x\,\mathrm{d}p_y\,\mathrm{e}^{-\beta H}\pi\bar{h}\delta(y)\delta(p_y) = \sqrt{\frac{1}{8\pi\beta\bar{h}^2}}\int \mathrm{d}x. \tag{2.2}$$

Since the x integral runs from $-\infty$ to ∞, this integral diverges even more violently than (2.1). We will also return to consider this more carefully below. The remaining three class heat kernels are well behaved. For the reflection through the diagonal axis σ_1, we change variables to $\xi = (x+y)/\sqrt{2}$ and $\eta = (x-y)/\sqrt{2}$ so that

$$\begin{aligned} Z(\sigma_1;\beta) &\approx \frac{1}{(2\pi\bar{h})^2}\int \mathrm{d}\xi\,\mathrm{d}\eta\,\mathrm{d}p_\xi\,\mathrm{d}p_\eta\,\mathrm{e}^{-\beta H}\pi\bar{h}\delta(\eta)\delta(p_\eta) \\ &= \frac{\Gamma(\frac{1}{4})}{4\sqrt{\pi}}\frac{1}{\beta^{3/4}\bar{h}}. \end{aligned} \tag{2.3}$$

The kernels corresponding to rotations by $\pi/2$ and π are trivial since all integrals are done by delta functions leaving

$$Z(R_{\pi/2};\beta) \approx \tfrac{1}{2} \qquad Z(R_\pi;\beta) \approx \tfrac{1}{4}. \tag{2.4}$$

We now go back and analyse, in greater detail, the first two integrals. The first was studied by Tomsovic [13] but for completeness and consistency of notation, we review the calculation.

Deep in one of the channels, $x \gg 1$ for example, the theory using the Wigner transforms breaks down due to the correction terms which are arbitrarily large. This can also be

understood as follows. Truncating (1.7) at its leading term involves an assumption that for short times one is free to ignore the dynamics so that the calculation involves only the local value of the Hamiltonian. Usually this is not problematic, however, for the present potential the channel effects violate that assumption; in one of the channels, $x \gg 1$ for example, we can treat the problem adiabatically so that in the y-direction there is harmonic motion with a frequency of $\omega_x = \sqrt{2}x$. This frequency can be arbitrarily large and there is no time scale over which the dynamics can be ignored. We overcome this problem by using an alternate representation of the heat kernels based on the adiabaticity of the problem as introduced in [13]. This is a complementary representation which is valid deep in the channels but fails near the origin. We assume that there is a domain of x where both representations are valid. Let Q be a value of x in this domain. For the adiabatic representation to be valid it must meet the condition that to be deep in one of the channels, in terms of dimensionless quantities this is $\Lambda = \beta^{1/4}Q \gg 1$. The condition for the Wigner function representation to be valid is $\epsilon = \beta\overline{h}Q \ll 1$. These conditions are compatible if $\beta^{3/4}\overline{h} \ll 1$. Determining all quantities in units of energy (E), Q has units of ($E^{1/4}$), β has units of (E^{-1}) and $\overline{h}$ has units of ($E^{3/4}$) so that all the conditions mentioned are in terms of-dimensionless combinations.

We will use the Wigner representation in the square $|x| \leqslant Q$, $|y| \leqslant Q$ and the adiabatic representation elsewhere. In analogy to (2.1), we define

$$Z_0(I;\beta) = \frac{1}{(2\pi\overline{h})^2}\frac{2\pi}{\beta}\int_{-Q}^{Q} \mathrm{d}x\,\mathrm{d}y\,\mathrm{e}^{-\beta x^2 y^2}. \tag{2.5}$$

We have introduced the subscript 0 to denote that this is the contribution from the central region around the origin. This integral can be calculated by the change of variables $u = \sqrt{\beta}xy$ and $v = x$, so that the integrand is proportional to $\exp(-u^2)/v$. Calculating the v integral first and using $\Lambda \gg 1$, one finds

$$Z_0(I;\beta) \approx \sqrt{\frac{1}{\pi\beta^3\overline{h}^4}}\left(\log(2\sqrt{\beta}Q^2) + \frac{\gamma}{2}\right) \tag{2.6}$$

where $\gamma = 0.5772\ldots$ is Euler's constant. Similarly, for the reflection operator σ_y, integration of (2.2) between the limits $-Q$ and Q leads to

$$Z_0(\sigma_y;\beta) = \sqrt{\frac{1}{2\pi\beta\overline{h}^2}}\,Q. \tag{2.7}$$

To do the integrals in the channels we assume a local separation of the Hamiltonian into a free particle in the x-direction and a harmonic oscillator in the y-direction, with a frequency which depends parametrically on x

$$h_x = \frac{1}{2}p_y^2 + \frac{\omega_x^2}{2}y^2. \tag{2.8}$$

Henceforth, we will use small letters to denote objects related to the local Hamiltonian h_x. It has eigenenergies $e_n = (n + \frac{1}{2})\omega_x\overline{h}$ and eigenstates $|\phi_n\rangle$ which depend parametrically on x. All the symmetry information concerned with the channel calculation is encoded in these

Table 2. Character table of the parity group.

	I	σ_y
E	1	1
O	1	−1

local eigenenergies and eigenstates. In particular, we are interested in the subgroup of C_{4v} which leaves x invariant and so maps the local eigenstates onto one another. This subgroup is just the parity group with group elements $\{I, \sigma_y\}$. For completeness we include its trivial character table as table 2. For fixed x, we proceed in analogy to (1.10) by defining heat kernels based on the local eigenvalues and corresponding to these two group operations,

$$\begin{aligned} z_x(g,\beta) &= \mathrm{Tr}(\hat{U}^\dagger(g)\mathrm{e}^{-\beta\hat{h}}) \\ &= \sum_n \eta_n(g)\mathrm{e}^{-\beta e_n} \end{aligned} \tag{2.9}$$

where g is either the identity or the reflection element. The trace operator 'Tr' denotes the local integral over the y degree of freedom and can be found by summing over the index n. It is clear that the operator $\hat{U}^\dagger(g)$ is unity when $g = I$ and changes the sign of the odd states when $g = \sigma_y$, so that $\eta_n(I) = 1$ and $\eta_n(\sigma_y) = (-1)^n$.

To evaluate the full trace, we note that the integrals in p_y and y have already been done implicitly in (2.9) so we only need to do the x and p_x integrals. Since this is only one-dimensional, the prefactor of the integral has only one power of $2\pi\hbar$ and we conclude

$$\begin{aligned} Z_c(g;\beta) &= \frac{f_g}{2\pi\hbar}\sum_n \eta_n(g)\int_{-\infty}^{\infty}\mathrm{d}p_x\int_Q^{\infty}\mathrm{d}x\,\mathrm{e}^{-\beta(p_x^2/2+(2n+1)\hbar x/\sqrt{2})} \\ &= f_g\sqrt{\frac{1}{\pi\beta^3\hbar^4}}\sum_n \eta_n(g)\frac{\xi^{2n+1}}{2n+1} \end{aligned} \tag{2.10}$$

where we have defined the factor $\xi = \exp(-\beta\hbar Q/\sqrt{2})$. (We include a subscript c to denote that this is the channel contribution.) We have also introduced a factor f_g which represents the number of channels which map to themselves under the action of the group element g. When working with the identity element, all the channels map onto themselves and $f_I = 4$; when working with the reflection operator σ_y, the channels along the x-axis map onto themselves and $f_{\sigma_y} = 2$. We now make use of the series identities

$$\begin{aligned} \sum_n \frac{\xi^{2n+1}}{2n+1} &= \frac{1}{2}\log\left(\frac{1+\xi}{1-\xi}\right) = -\frac{\log\epsilon}{2} + \frac{\log 2}{2} + \frac{\epsilon^2}{24} + \mathrm{O}(\epsilon^4) \\ \sum_n (-1)^n\frac{\xi^{2n+1}}{2n+1} &= \arctan\xi = \frac{\pi}{4} - \frac{\epsilon}{2} + \frac{\epsilon^3}{12} + \mathrm{O}(\epsilon^5) \end{aligned} \tag{2.11}$$

where we recall $\epsilon = \beta\hbar Q \ll 1$. Using just the first two terms (we return to the third term later) we conclude

$$\begin{aligned} Z_c(I;\beta) &\approx -\sqrt{\frac{1}{\pi\beta^3\hbar^4}}\log\left(\frac{\hbar^2\beta^2Q^2}{8}\right) \\ Z_c(\sigma_y;\beta) &\approx \sqrt{\frac{\pi}{4\beta^3\hbar^4}} - \sqrt{\frac{1}{2\pi\beta\hbar^2}}Q. \end{aligned} \tag{2.12}$$

We add the results from the centre (2.6) and (2.7) to the channel results (2.12) to find

$$\begin{aligned} Z(I;\beta) &\approx \sqrt{\frac{1}{4\pi\beta^3\hbar^4}}\left(\log\left(\frac{1}{\beta^3\hbar^4}\right) + \gamma + 8\log 2\right) \\ Z(\sigma_y;\beta) &\approx \sqrt{\frac{\pi}{4\beta^3\hbar^4}}. \end{aligned} \tag{2.13}$$

Note that the Q dependence has cancelled from both results leaving a finite answer. (This prescription actually overcounts some regions of phase space but the errors so introduced are exponentially small in Λ.)

We have now calculated the five class heat kernels which we need. All that remains is to compute their inverse Laplace transforms. In fact, we will not be interested in the densities $\rho(g; E)$ themselves but rather in their integrals $N(g; E)$ which are given by

$$N(g; E) = \mathcal{L}^{-1}\left(\frac{Z(g; \beta)}{\beta}\right). \tag{2.14}$$

The inverse Laplace transforms are

$$\begin{aligned} N(I; E) &\approx \frac{2}{3\pi} y^2(4\log y + 4\gamma + 14\log 2 - 8) \\ N(\sigma_y; E) &\approx \tfrac{2}{3} y^2 \\ N(\sigma_1; E) &\approx \frac{\Gamma^2(\frac{1}{4})}{\sqrt{18\pi^3}} y \\ N(R_{\pi/2}; E) &\approx \tfrac{1}{2} \\ N(R_\pi; E) &\approx \tfrac{1}{4}. \end{aligned} \tag{2.15}$$

We have defined the-dimensionless scaled energy $y = E^{3/4}/\overline{h}$, which is a semiclassically large quantity. If we explicitly include the mass m in the kinetic energy of the Hamiltonian and a parameter α in front of the potential energy then equation (2.15) still applies but with $y = (m^{1/2}E^{3/4})/(\alpha^{1/4}\overline{h})$. To construct the integrated densities of states for each of the five irreps, we adapt equation (1.11) by replacing the symbols Z with the symbols N,

$$N_R(\beta) = \frac{d_R}{|G|}\sum_g \chi_R^*(g) N(g; \beta) \tag{2.16}$$

which written out explicitly is

$$\begin{pmatrix} N_{A1}(E) \\ N_{A2}(E) \\ N_{B1}(E) \\ N_{B2}(E) \\ N_E(E) \end{pmatrix} = \frac{1}{8}\begin{pmatrix} 1 & 2 & 2 & 2 & 1 \\ 1 & -2 & 2 & -2 & 1 \\ 1 & 2 & -2 & -2 & 1 \\ 1 & -2 & -2 & 2 & 1 \\ 4 & 0 & 0 & 0 & -4 \end{pmatrix}\begin{pmatrix} N(I; E) \\ N(\sigma_y; E) \\ N(\sigma_1; E) \\ N(R_{\pi/2}; E) \\ N(R_\pi; E) \end{pmatrix}. \tag{2.17}$$

We further note that the inverse Laplace transforms imply that all the functions are zero for negative energies. The first of the relations (2.15) is the average integrated density of states summed over all irreps as found by Tomsovic [13]. These are just the leading order results in an asymptotic semiclassical expansion, however, we will show in section 4 that they are good up to and including terms in $O(1/y)$. Additionally, these results are consistent with unpublished results [9, 23].

For typical two-dimensional potentials with finite phase space volumes, the term $N(I; E)$ scales as $1/\overline{h}^2$. The prefactor of that term in (2.15) has this scaling but there is a further logarithmic dependence on $\overline{h}$ which causes it to grow somewhat faster. This logarithmic factor arises from the fact that the integral in (2.5) diverges logarithmically with Q. One must be careful in discussing 'orders' when expressions involve logarithms of large quantities and for practical purposes, the non-logarithmic term $4\gamma + 14\log 2 - 8$ represents an essential correction, as discussed in [13]. Based on equation (1.8), we expect terms involving reflection operators to be weaker by a relative power of $\overline{h}$ and therefore to scale as $1/\overline{h}$. This is not true for $N(\sigma_y; E)$ which is amplified by a factor of $1/\overline{h}$ so that it is of the same order as the non-logarithmic term in $N(I; E)$. The fact that it has been

amplified by a full power of $1/\overline{h}$ can be traced to the fact that the integral (2.2) diverges linearly with Q. Therefore, rather than being a relatively weak correction, this reflection operator is almost leading order in its effect. In particular, the approximate relation that the fraction of states in irrep R is approximately $d_R^2/|G|$ fails in general, since it comes from considering just the identity operator. (However, it is valid for the E irrep which is independent of that reflection class.) A similar behaviour is also apparent in the related problem of the hyperbola billiard [24, 4]. The other reflection class function $N(\sigma_1; E)$ does scale as $1/\overline{h}$ as we expect for normal reflection operations. The two rotation classes also behave normally [17], being constants independent of $\overline{h}$.

3. Numerical comparison of two dimensional results

We numerically diagonalized the quantum Hamiltonian for each irrep by using appropriately symmetrized bases with 200 harmonic oscillator wavefunctions in both the x- and y-directions and with $\overline{h} = 1$. To make the comparison more explicit, we convolved the numerically obtained density of states by a Gaussian of width w,

$$\tilde{\rho}_R(E) = \frac{1}{\sqrt{2\pi w^2}} \sum_n \exp\left(-\frac{(E - E_n)^2}{2w^2}\right). \tag{3.1}$$

The integrated density of states is then obtained by replacing the sharp steps at the quantum eigenvalues by the corresponding error functions. For large w, this convolution washes out all oscillations leaving just the average behaviour.

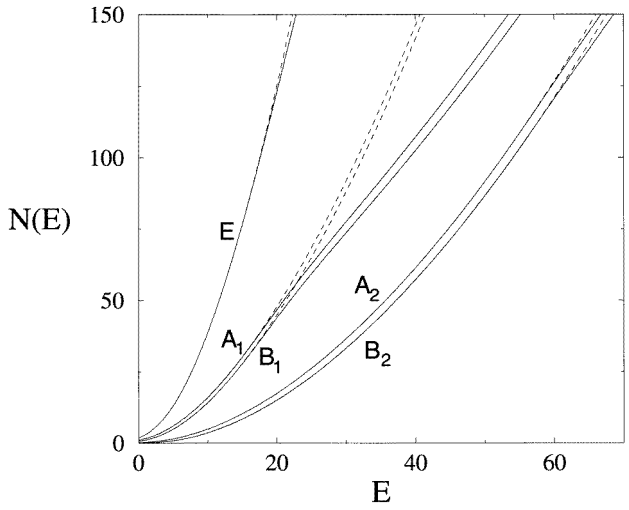

Figure 2. The full curves indicate the smoothed density of states for each of the five irreps as found numerically. The broken curves are the corresponding analytical forms derived in this paper.

In figure 2 we show the results for all five irreps with a smoothing width $w = 3$. The full curves are the numerics and the broken curves are the analytical forms. The first thing which is apparent is that there is a great distinction between the A_1 and B_1 states compared with the A_2 and B_2 states, resulting from the large contribution of $N(\sigma_y; E)$. Between each of these pairs there is a much smaller splitting due to $N(\sigma_1; E)$. The deviations between the full and broken curves are completely numerical in origin and arise from the finite

basis used in determining the quantum eigenvalues. Due to the channels, the eigenvalues converge very slowly with increased basis size. It is interesting to note that the irreps which are odd with respect to reflections through the channels are better converged. Being odd, they are less sensitive to the effects of the channels and are therefore less prone to error. Nevertheless, their error is still dominated by channel effects as we will demonstrate. The other three irreps are not odd with respect to both channels (A_1 and B_1 are even with respect to both channels and the E states can be chosen as even with respect to one and odd with respect to the other). All three of them fail at approximately the same energy of $E \approx 18$. The number of accurate eigenvalues is approximately 35 for A_1 and B_1 and 45 for E (recall that E is doubly degenerate so the number of independent eigenvalues obtained is half the number of states plotted). This is rather dismal considering the 40 000 oscillator states used. The irreps A_2 and B_2 are accurate up to energies near $E \approx 60$ representing approximately 115 states each.

It is also interesting to numerically isolate the contributions from the various classes and compare them with (2.15) directly as done in [17]. The matrix in (2.17) is readily inverted due to the orthonormal property of the characters with the result

$$\begin{pmatrix} N(I;E) \\ N(\sigma_y;E) \\ N(\sigma_1;E) \\ N(R_{\pi/2};E) \\ N(R_\pi;E) \end{pmatrix} = \begin{pmatrix} 1 & 1 & 1 & 1 & 1 \\ 1 & -1 & 1 & -1 & 0 \\ 1 & 1 & -1 & -1 & 0 \\ 1 & -1 & -1 & 1 & 0 \\ 1 & 1 & 1 & 1 & -1 \end{pmatrix} \begin{pmatrix} N_{A1}(E) \\ N_{A2}(E) \\ N_{B1}(E) \\ N_{B2}(E) \\ N_E(E) \end{pmatrix}. \tag{3.2}$$

This can be written compactly as

$$N(g;E) = \sum_R \eta_R(g) N_R(E) \tag{3.3}$$

where the factors $\eta_R(g)$ are defined in (3.2) and can be thought of as the inverse of the group characters. In figure 3 we plot $N(I;E)$, $N(\sigma_y;E)$ and $N(R_\pi;E)$ from the theory and with the numerical eigenvalues combined according to (3.2). As mentioned, the first is just the total number of states. The third is shown in its own panel since its value is of a very different scale than the other two. They all fail around $E \approx 18$ which is consistent with the previous figure. $N(R_\pi;E)$ depends on very fine cancellations and is more sensitive to small errors so it is consistent that it produces noticeable deviations at a slightly smaller energy than the other two. Equation (2.15) predicts a flat line for $N(R_\pi;E)$, the structure at smaller E comes from the convolution (3.1) which is applied to the analytical forms as well as to the numerical data.

The other two conjugacy classes behave very differently; we plot these results in figure 4. The upper panel shows $N(\sigma_1;E)$ and the lower panel shows $N(R_{\pi/2};E)$. For the lower panel, we choose two different smoothing widths, the relevance of which we discuss below. For now, consider the comparison between the smooth full curve and the broken curve in each case. The results are now accurate up to energies of $E \approx 800$ or more than 40 times the range observed in the previous figure. This indicates that the numerics are, in some sense, better than a quick study of figure 2 would indicate. Although the various irreps are individually prone to error even at relatively modest energies, these errors are very correlated so that appropriate combinations cause them to cancel. In fact, this is apparent in figure 2 since the pairs A_1 and B_1 and also A_2 and B_2 deviate from their expected behaviour in very correlated manners. From (3.2) we see that both $N(\sigma_1;E)$ and $N(R_{\pi/2};E)$ involve the differences $N_{A1}(E) - N_{B1}(E)$ and $N_{A2}(E) - N_{B2}(E)$ and the systematic effects cancel for these two classes. Since the numerics agree with these functions up to $E \approx 800$, it is reasonable to associate all the numerical errors with $N(I;E)$ and $N(\sigma_y;E)$, i.e. with the

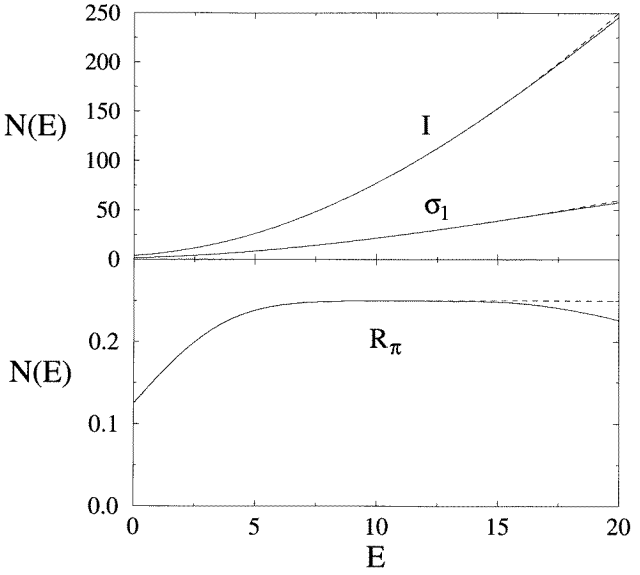

Figure 3. Top: the upper pair of curves indicates the function $N(I; E)$ which is the total density of states. The lower pair shows $N(\sigma_y; E)$. In each case the full curve comes from the numerics and the broken curve is the analytical form. Bottom: the same for $N(R_\pi; E)$.

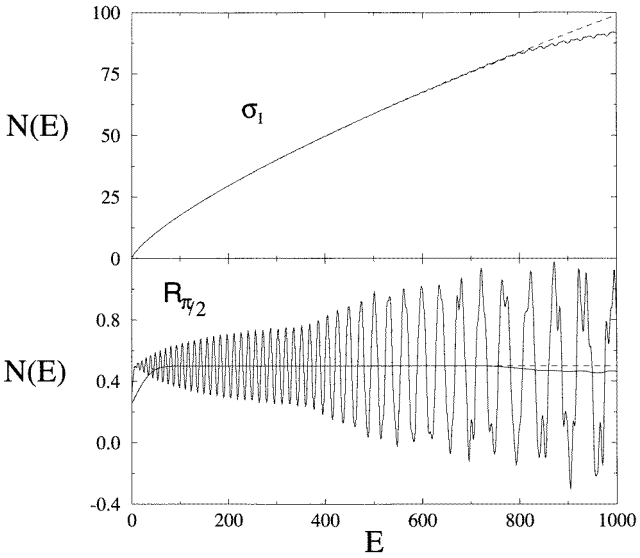

Figure 4. The same as the previous figure except that the upper panel indicates $N(\sigma_1; E)$ and the lower panel $N(R_{\pi/2}; E)$. The solid oscillating curve has with a smoothing width of 3. The other full curve and analytical broken curve have smoothing widths of 30.

channels. This is obviously true for the irreps A_1, B_1 and E, however, it is also true for the odd irres A_2 and B_2. Their staircase functions fail at $E \approx 60$ which is better than the other irreps but still very much smaller than the classes $N(\sigma_1; E)$ and $N(R_{\pi/2}; E)$.

We now briefly discuss the oscillatory structure visible in the bottom panel of figure 4. This type of structure was also observed in [17] where it was explained in terms of fractions of periodic orbits [25]. In this example, the structure arises from the square-like periodic orbit shown in figure 1. After completing one quarter of a cycle, the trajectory is related to its initial point by a rotation of angle $\pi/2$. This quarter-orbit then contributes an oscillatory contribution to the function $N(R_{\pi/2}; E)$. This is a scaling system whose classical mechanics is independent of energy, after appropriate scalings. In particular, the period of an orbit scales as $T \propto E^{-1/4}$ which explains the growing wavelength with energy. Additionally, the smoothing suppresses the oscillatory contribution by a factor proportional to $\exp(-w^2T^2/2)$ which explains why the amplitude of oscillation increases with energy. At the highest end of the energy range, one sees the contributions of higher repetitions—for example, three quarters of the square orbit will also contribute to $N(R_{\pi/2}; E)$. The function $N(R_{\sigma_1}; E)$ receives contributions from fractional orbits which map to themselves under reflection through the diagonal. Examples of this include the diagonal orbit after a half period and after a full period. Such structure is visible at the upper end of the energy range but is less apparent than in the bottom panel because of the different vertical scale.

A similar structure also exists for the other classes but it is not visible due to the short energy range available. $N(R_\pi; E)$ receives contributions from one half of the diagonal orbit and one half of the square orbit. $N(\sigma_y; E)$ receives a strong contribution from the almost periodic family of orbits corresponding to the adiabatic oscillation deep in the channels (actually, from the fractional periodic family which has one half the period). This is a non-standard contribution due to the intermittency, such effects are discussed in [4–7]. The function $N(I; E)$ receives contributions from all the complete orbits but not from any fraction of them. The periodic orbit theory of this system has been discussed in detail in [5] and the references therein, so we forego a more detailed discussion.

We conclude by applying the expansions to develop a crude semiclassical quantization of the system. The true quantum staircase functions change discontinuously from one integer value to the next at the energy eigenvalues. Any finite approximation to this staircase function will induce a smoothing so that there are no exact discontinuities; we then estimate eigenvalues by where the approximate staircase function passes through half-integer values. In particular, this quantization condition reproduces the eigenvalues in the limit that the approximation approaches the true staircase. We use this algorithm with the integrated Thomas–Fermi density of states as the approximation. This is an admittedly poor way to estimate quantum energies but we include a discussion for two reasons. The first is that it serves as a benchmark for other semiclassical quantization schemes. Another approximation is particularly useful if it can give numbers which are significantly better than those from the Thomas–Fermi quantization. For example, in table 3 we also show the results of a recent

Table 3. The first three exact quantum energies of each irrep (ex) compared to the quantization from the integrated Thomas–Fermi density of states (tf) and the semiclassical results of [11] (sc).

	1					2					3				
	A_1	A_2	B_1	B_2	E	A_1	A_2	B_1	B_2	E	A_1	A_2	B_1	B_2	E
ex	0.698	3.157	1.925	5.087	1.498	2.214	5.842	2.994	7.227	2.579	3.140	7.415	3.871	8.958	3.464
tf	0.881	3.438	1.856	5.147	1.573	2.196	5.728	3.037	7.353	2.628	3.131	7.364	3.935	8.959	3.405
sc	0.612	3.077	1.889	4.996	1.460	2.278	5.769	2.705	7.115	2.408	2.697	6.669	3.888	8.404	3.000

Table 4. The first 12 exact quantum energies compared to the quantization from the individual Thomas–Fermi terms for each irrep (tf) and to the quantization from the total integrated Thomas–Fermi density of states (tf') without regard to symmetry decomposition.

	1	2	3	4	5	6	7	8	9	10	11	12
	$A1$	E	E	$B1$	$A1$	E	E	$B1$	$A1$	$A2$	E	E
ex	0.698	1.498	1.498	1.925	2.214	2.579	2.579	2.994	3.140	3.157	3.464	3.464
tf	0.881	1.573	1.573	1.856	2.196	2.628	2.628	3.037	3.131	3.438	3.405	3.405
tf'	0.795	1.296	1.656	1.957	2.221	2.461	2.682	2.889	3.085	3.271	3.448	3.619

quantization based on a semiclassical treatment of the heat kernel using imaginary time trajectories [11]. (Note that they used $V = x^2y^2/2$ so that their energies have been scaled by $2^{1/3}$ for a comparison with the convention of this paper. Also, their definitions of A_2 and B_2 are switched relative to those here.) Their treatment typically captures the ground-state energies better, but the Thomas–Fermi quantization is usually better for the first two excited states. This implies that their method is most effective for the ground state and less so for higher excited states—in agreement with their own conclusions. For completeness, we also mention that Martens *et al* [10] used an adiabatic separation together with a semiclassical approximation to achieve much higher accuracy but at the price of incorrectly predicting too many degeneracies such that their results only work well after averaging.

The second reason for considering the Thomas–Fermi quantization is to provide an example of the importance of symmetry decompositions. In table 4, we compare the results using the Thomas–Fermi formulae for the separate irreps $N_R(E)$ with the total density of states $N(I; E)$. The results for the first 12 states, as sorted by energy independently of irrep, are presented in table 4. Numerically, the quantization using $N(I; E)$ is competitive but it has two serious draw backs. The first is that even for those states which are well reproduced, we have no way of knowing to which irrep to assign them without the symmetry decomposition. Secondly, by definition it cannot reproduce correctly the two-fold degeneracy associated with the E states—this degeneracy is implicit in the quantization based on the individual irreps.

4. Higher-order considerations

It was stated in section 2 that the results quoted are accurate up to and beyond constant terms. We will now demonstrate this by discussing the corrections to each of the class functions. The discussion will be based on keeping the next order term in the relation (1.7). The approach is to insert this expanded version into the trace integral (1.6) together with the Wigner transform of the group element under consideration (1.8) to get the higher-order corrections to each class. We first dispense with the two rotational classes. Upon inverse Laplace transforming, the various powers of β correspond to derivatives as a function of energy—which can be brought outside of the phase-space integral used in calculating the trace. However, the resulting phase-space integral is independent of energy (except at $E = 0$) due to the delta functions in the coordinates and momenta. Thus, there is no contribution at finite energy. This is true to all orders in both expansions (1.7) and (1.8). This point is discussed more extensively in [17]. We conclude, therefore, that the two rotation classes do not have higher-order corrections at non-zero energies.

The expansion (1.7) is in even powers of $\overline{h}$ so we would expect that the remaining three classes have corrections of order $\overline{h}^2$ relative to their leading-order behaviour. This would

imply constant terms for the identity and the channel reflection and a term of order $1/y$ for the other reflection, σ_1. In fact, for different reasons, none of these are realized. For the reflection class σ_1, the correction of order $1/y$ vanishes, as we will show below. For identity and the channel reflection, the expansion is actually in powers of $\overline{h}^4$, not $\overline{h}^2$, so the first corrections are two powers of $\overline{h}$ weaker than one would expect (ignoring possible logarithmic dependencies [13]) and in this case the $O(\overline{h}^4)$ in (1.7) should read $O(\overline{h}^8)$.

Starting with the reflection class σ_1, we use the coordinates ξ and η as in (2.4) and introduce the expansion (1.7) into the trace integral. The presence of the delta functions in η means that we only need to explicitly determine the various terms in (1.7) as functions of ξ. Noting that $V = (\xi^2 - \eta^2)^2/4$, one finds

$$\nabla^2 V|_{\eta=0} = 2\xi^2 \qquad (\boldsymbol{\nabla} V)^2|_{\eta=0} = \xi^6 \qquad (\boldsymbol{p}\cdot\boldsymbol{\nabla})^2 V|_{\eta=p_\eta=0} = 3p_\xi^2\xi^2. \tag{4.1}$$

The first of these contributes to $Z(\sigma_1;\beta)$ an amount

$$\frac{\pi\overline{h}}{(2\pi\overline{h})^2}\int \mathrm{d}p_\xi\,\mathrm{d}\xi\,\mathrm{e}^{-\beta(p_\xi^2/2+\xi^4/4)}\left(-\frac{\overline{h}^2\beta^2}{8}\nabla^2 V\right) = -\frac{\Gamma(\frac{3}{4})}{8\sqrt{\pi}}\beta^{3/4}\overline{h}. \tag{4.2}$$

The other two correction integrals are equal to each other and are one half in magnitude to the first. Due to the relative sign, the sum of the three cancels identically and there is no contribution to this order. The next-order contribution is at most $O(y^3)$. It is amusing to note that if we take $V = \xi^4/4$ and repeat the calculation in one dimension then $\nabla^2 V = 3\xi^2$ while the other two terms are unchanged. The terms do not balance and we obtain a non-zero result. We conclude that in spite of the delta functions, the second degree of freedom plays an important role for the reflection classes.

For the remaining two classes, identity and σ_y, we do not present the detailed calculations but rather argue that the corrections are smaller than constant y^0 terms as stated in [13]. There are various sources of correction: the higher-order analysis in the region around the origin; the higher-order analysis in the channels; the higher-order terms in the expansions (2.11); the parametric x-dependence of the adiabatic eigenstates $|\phi_n\rangle$; and, corrections from the Baker–Campbell–Hausdorff expansion $\exp(-\beta(p_x^2/2+p_y^2/2+x^2y^2)) \approx \exp(-\beta p_x^2/2)\exp(-\beta(p_y^2/2+x^2y^2))$ implicit in the adiabatic calculation. Each of these give corrections which are, in principle, dependent on the parameter Q. However, term by term the Q-dependence must vanish, as we have seen above, leaving factors independent of Q. For example, the higher-order corrections in the region around the origin give factors which grow quadratically and cubically with Q for the identity and σ_y respectively. This fact is in accordance with the discussion in the opening paragraph of section 2 where it was stated that the correction terms are arbitrarily large. However, these terms are cancelled by the third terms in the expansions (2.11). In fact, all correction terms which behave as $\overline{h}^0$ are Q-dependent and must be cancelled.

As an example of higher-order terms which are not Q-dependent, we consider the contribution to the corrections arising from the channel calculations. Each of the terms in the sum (2.10) can be thought of as arising from an effective Hamiltonian in x given by

$$H_n^{\mathrm{eff}} = \frac{p_x^2}{2} + \frac{(2n+1)}{\sqrt{2}}\overline{h}x. \tag{4.3}$$

The effective potentials have two important properties, they are proportional to $\overline{h}$ and they are linear in x. The first implies that the expansion (1.7) will involve higher powers of $\overline{h}$. The linearity in x implies that the only non-zero correction term is

$$(\boldsymbol{\nabla} V)^2 = \frac{(2n+1)^2}{2}\overline{h}^2. \tag{4.4}$$

so that the correction to (2.10) is

$$Z_c^{\rm corr}(g;\beta) = \frac{f_g}{48\sqrt{\pi}}\beta^{3/2}\overline{h}^2\sum_n \eta_n(g)(2n+1)\xi^{2n+1}. \tag{4.5}$$

We now make use of the series identities

$$\begin{aligned}\sum_n (2n+1)\xi^{2n+1} &= \frac{\xi(1+\xi^2)}{(1-\xi^2)^2} = \frac{1}{\epsilon^2}+\frac{1}{12}+{\rm O}(\epsilon^2)\\ \sum_n (-1)^n(2n+1)\xi^{2n+1} &= \frac{\xi(1-\xi^2)}{(1+\xi^2)^2} = 0+{\rm O}(\epsilon)\end{aligned} \tag{4.6}$$

where we use $\epsilon = \beta\overline{h}Q \ll 1$. Reintroducing the prefactor of (4.5), we conclude that up to constant terms in (4.6), the corrections from the channel calculation are

$$Z_c^{\rm corr}(I;\beta) \approx \frac{1}{12\sqrt{\pi}\Lambda^2}+\frac{\beta^{3/2}\overline{h}^2}{144\sqrt{\pi}} \qquad \text{and} \qquad Z_c^{\rm corr}(\sigma_y;\beta)\approx 0. \tag{4.7}$$

We are most interested in the second term of the first equation since it is independent of Q. Taking its inverse Laplace transform implies a contribution of $-1/(288\pi y^2)$ to the identity class which is four powers of $\overline{h}$ weaker than the leading term. We do not claim that this is the only contribution to the correction but do claim that it is representative in its $\overline{h}$ dependence. The correction terms to both the identity and σ_y classes are weaker than $1/y$. In [13] the author states the correction for the identity actually behaves as $\log y/y^2$.

One has the freedom to consider an exponentiated version of (1.7) in which the corrections are in the exponential [15]. It turns out that the correction term $\nabla^2 V$ then regularizes the resulting integrals [26]. However, this leads to results which are not the same as what one finds using the adiabatic separation in the channels. For example, for the reflection element σ_y, the integral to be done is

$$\frac{\pi\overline{h}}{(2\pi\overline{h})^2}\int_{-\infty}^{\infty}{\rm d}x\,{\rm d}p_x\,{\rm e}^{-\beta p_x^2/2-\beta^2\overline{h}^2x^2/4} = \sqrt{\frac{1}{2\beta^3\overline{h}^4}} \tag{4.8}$$

which is obviously not in agreement with $Z(\sigma_y;\beta)$ of (2.13). The reason for the disagreement is that the x integral in (4.8) cuts off at values of order $x\sim 1/\overline{h}\beta$. However, at this value of x the higher-order corrections have similar numerical values and it is inconsistent to neglect them. In contrast, using the adiabatic separation we only evaluate the integral out to a value $Q \ll 1/\overline{h}\beta$ and it is consistent to neglect higher-order terms.

All of the conclusions of this section about the higher-order corrections are consistent with the numerical data [27]. However, since all the corrections are small it was impossible to actually extract any of them numerically. It should also be mentioned that the various expansions are asymptotic and typically diverge in a manner controlled by the shortest periodic orbits in the system [28]. In this case, however, one could imagine that it is rather the adiabatic separation which controls the divergence of the series. This would be an interesting issue to explore, however, the proliferation of contributions to the correction terms make this a rather difficult series to expand. On the other hand, the fact that it is apparently a series in $\overline{h}^4$ might mean that fewer terms need to be evaluated before the divergence manifests itself.

5. The three-dimensional generalization

In this section we discuss the three-dimensional potential $V = x^2y^2+y^2z^2+z^2x^2$. This is the potential which actually appears in the zero-dimensional limit of the $SU(2)$ Yang–

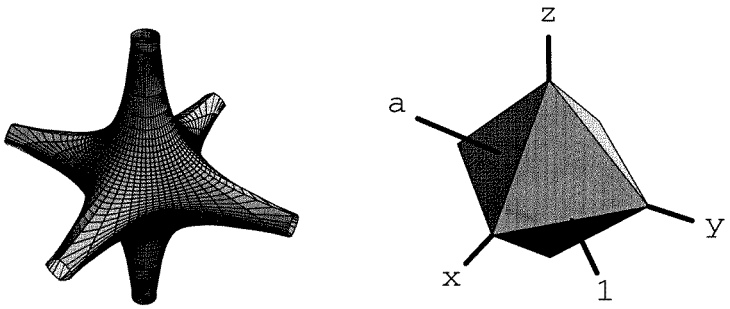

Figure 5. Left: an equal energy contour of the three-dimensional potential $V = x^2y^2 + y^2z^2 + z^2x^2$ showing the six channels along the three axes. Right: an octahedron with the relevant points labelled for the description of the group elements.

Mills equations. The symmetry group is that of the octahedral group in which we allow spatial inversions—the extended octahedral group. In figure 5 we show a three-dimensional constant energy contour of the potential and also an octahedron whose vertices are aligned along the channel directions. In total there are 48 group elements organized into 10 conjugacy classes. This group is the direct product of the inversionless octahedral group and the inversion parity group. The first of these is composed of 24 group elements organized into five classes [29] and we start by enumerating these. First, there is the identity I, which is in a class by itself. There is a class of six elements involving rotations by $\pm\pi/2$ about any of the three axes, such as $R_{x,\pi/2}$. Similarly, there is a class of three elements involving rotations by π about these axes, for example $R_{x,\pi}$. There is a class of eight elements involving rotation by $\pm 2\pi/3$ about any of the face–face axes, such as $R_{a,2\pi/3}$. Finally, there is a class of six elements involving rotations by π about any of the the six edge–edge axes, such as $R_{1,\pi}$. We refer to these classes as C_1 to C_5 respectively. This group has five irreps and the character table is the top left quarter of table 5.

To construct the full group, we multiply representative members of each class by the inversion operation $\Sigma = \sigma_x\sigma_y\sigma_z$. The effect of this is to map the identity to the inversion element Σ and to map each rotation into either a single reflection or into a rotation times a reflection; this induces five additional classes. The element Σ is in a class by itself.

Table 5. Character table of the extended octahedral group. The number in brackets at the top of each column indicates the number of group elements which belong to that class. Representative members of the various classes are described in the text.

	C_1 (1)	C_2 (6)	C_3 (3)	C_4 (8)	C_5 (6)	C_1' (1)	C_2' (6)	C_3' (3)	C_4' (8)	C_5' (6)
Γ_1	1	1	1	1	1	1	1	1	1	1
Γ_2	1	−1	1	1	−1	1	−1	1	1	−1
Γ_3	2	0	2	−1	0	2	0	2	−1	0
Γ_4	3	−1	−1	0	1	3	−1	−1	0	1
Γ_5	3	1	−1	0	−1	3	1	−1	0	−1
Γ_1'	1	1	1	1	1	−1	−1	−1	−1	−1
Γ_2'	1	−1	1	1	−1	−1	1	−1	−1	1
Γ_3'	2	0	2	−1	0	−2	0	−2	1	0
Γ_4'	3	−1	−1	0	1	−3	1	1	0	−1
Γ_5'	3	1	−1	0	−1	−3	−1	1	0	1

Composition of the second class with Σ gives a class of six elements which are rotations by $\pm\pi/2$ through an axis times reflection through that axis, such as $R_{x,\pi/2}\sigma_x$. Composition of the third class with Σ gives the reflection elements about the three planes, such as σ_x. The fourth class becomes a product of a rotation about a face–face axis times a reflection through the perpendicular plane, such as $R_{a,2\pi/3}\sigma_a$. Finally, the fifth class becomes reflections through planes defined by the edges and vertices. An example is the plane defined by the point 1 together with the vertices at positive and negative z. We call reflections through this plane σ_1. We denote these five additional classes C_1'–C_5' respectively. The addition of these classes doubles the number of irreps and the full character table is shown in table 5.

We recall that in the two-dimensional problem we needed to consider the subgroup which mapped a single channel onto itself—in that case it was the parity group; we do the same here. The eight group elements which map the channel $x \gg 1$ (for example) onto itself are I, $\sigma_{y,z}$, $\sigma_{2,3}$, $R_{x,\pm\pi/2}$ and $R_{x,\pi}$ and these belong to classes C_1, C_3', C_5', C_2 and C_3 respectively. ($\sigma_{2,3}$ are defined in analogy to σ_1; they are reflections through the two planes defined by the vertices at positive and negative x and the midpoints of the two edges connecting the z-vertex to the positive and negative y-vertices.) We can expect the integrals associated with these elements to be problematic and to possibly require the adiabatic matching used in section 3. Together these eight elements comprise the subgroup C_{4v} which is, of course, the group we studied in the two-dimensional problem.

In all calculations of this section, we work only to leading order in $\hbar$. We start by studying the five classes which do not require an adiabatic analysis. The class C_1' involves three orthogonal reflections while the classes C_2' and C_4' involve rotations and perpendicular reflections. Their Wigner transforms are given by (1.9) and are trivial to integrate since they involve delta functions of all the quantities. Their contributions are $\frac{1}{8}$, $\frac{1}{4}$ and $\frac{1}{6}$ respectively. The class C_4 involves rotations through the face axes. For rotation by $2\pi/3$ through the point a, we define a change of variables

$$\xi = \frac{1}{\sqrt{3}}(x - y + z) \qquad \eta = \frac{1}{\sqrt{6}}(2x + y - z) \qquad \zeta = \frac{1}{\sqrt{2}}(y + z) \tag{5.1}$$

so that the potential along the ξ-axis is $V = \xi^4/3$. We then use the third equation of (1.8) with this choice of variables to find

$$Z(C_4; \beta) \approx \frac{\Gamma(\frac{1}{4})}{\sqrt{24\sqrt{3}\pi}} \frac{1}{\beta^{3/4}\hbar}. \tag{5.2}$$

For rotation by π through the point 1, we define a change of variables

$$\xi = \frac{1}{\sqrt{2}}(x + y) \qquad \eta = \frac{1}{\sqrt{2}}(x - y) \qquad \zeta = z \tag{5.3}$$

so that the potential along the ξ-axis is $V = \xi^4/4$. We then find

$$Z(C_5; \beta) \approx \frac{\Gamma(\frac{1}{4})}{8\sqrt{\pi}} \frac{1}{\beta^{3/4}\hbar}. \tag{5.4}$$

We now consider the more interesting classes which map at least one channel onto itself. We earlier suggested that the integrals corresponding to them might be problematic. In fact, this is true for all of them except the identity whose integral converges without such an analysis. Therefore, we do it first,

$$\begin{aligned} Z(I; \beta) &\approx \frac{1}{(2\pi\hbar)^3} \int \mathrm{d}x\, \mathrm{d}y\, \mathrm{d}z\, \mathrm{d}p_x\, \mathrm{d}p_y\, \mathrm{d}p_z\, \mathrm{e}^{-\beta H} \\ &= \frac{\Gamma^3(\frac{1}{4})}{\sqrt{32\pi^3}} \frac{1}{\beta^{9/4}\hbar^3}. \end{aligned} \tag{5.5}$$

(The p integrals are done trivially and the spatial integrals can be done by use of cylindrical coordinates.) The convergence of this integral is due to the fact that deep in one of the channels, the energetically accessible area pinches off as $1/x^2$, which is integrable. The analogous integral in two-dimensions pinches off as $1/x$ and is not integrable.

For reflection in z, which is a member of the C_3' class, we use equation (1.8) inside a cube $|x| \leqslant Q$, $|y| \leqslant Q$ and $|z| \leqslant Q$ and so define the following integral,

$$Z_0(\sigma_z;\beta) = \frac{1}{2}\frac{1}{(2\pi\hbar)^2}\int_{-\infty}^{\infty} \mathrm{d}p_x\,\mathrm{d}p_y\,\mathrm{e}^{-\beta(p_x^2+p_y^2)/2}\int_{-Q}^{Q}\mathrm{d}x\,\mathrm{d}y\,\mathrm{e}^{-\beta x^2 y^2}. \tag{5.6}$$

Other than the factor of one half, this is the same integral we evaluated to get the total density of states in the two-dimensional problem. The result is given by (2.6) so that

$$Z_0(\sigma_z;\beta) \approx \sqrt{\frac{1}{\pi\beta^3\hbar^4}}\left(\log Q + \log\beta^{1/4} + \frac{\gamma}{4} + \frac{1}{2}\log 2\right). \tag{5.7}$$

Reflection in σ_3, which is a member of the C_5' class, requires a more complicated calculation. We define a change of coordinates so that $\eta = (z+y)/\sqrt{2}$ and $\zeta = (z-y)/\sqrt{2}$ and then use equation (1.8) with the delta functions acting on ζ and p_ζ so that the integral to be evaluated is

$$Z_0(\sigma_3;\beta) = \frac{1}{\pi\beta\hbar^2}\int_0^Q \mathrm{d}x\int_0^{\sqrt{2}Q}\mathrm{d}\eta\,\mathrm{e}^{-\beta(x^2\eta^2+\eta^4/4)}. \tag{5.8}$$

We have done the trivial momentum integrals and have noted that by its definition, η has a different integration range than x. This integral can be done in a manner analogous to (2.5), we define integration variables $u = x\eta$ and $v = \eta$. Doing the v integration first and using $\beta^{1/4}Q \gg 1$ one arrives at

$$Z_0(\sigma_3;\beta) \approx \sqrt{\frac{1}{4\pi\beta^3\hbar^4}}\left(\log Q + \log\beta^{1/4} + \frac{\gamma}{4} + \frac{3}{2}\log 2\right). \tag{5.9}$$

Rotation by $\pi/2$ about the x-axis is a member of the C_2 class and implies delta functions in the other two variables so that the integral to be done is

$$\begin{aligned} Z_0(R_{\pi/2};\beta) &= \frac{1}{4\pi\hbar}\int_{-\infty}^{\infty}\mathrm{d}p_x\,\mathrm{e}^{-\beta p_x^2/2}\int_{-Q}^{Q}\mathrm{d}x \\ &= \sqrt{\frac{1}{2\pi\beta\hbar^2}}\,Q. \end{aligned} \tag{5.10}$$

Rotation by π about the x-axis, which is a member of the C_3 class, involves an integral which is identical except for a factor of two from the $\sin^2(\theta/2)$ factor in (1.8). Therefore

$$Z_0(R_\pi;\beta) = \sqrt{\frac{1}{8\pi\beta\hbar^2}}\,Q. \tag{5.11}$$

6. Channel calculations in three-dimensions

In this section we evaluate the contribution of the channels in three dimensions. As discussed before, this is is only necessary for some of the group elements. In analogy with (2.8) we define a local two-dimensional Hamiltonian as

$$h_x = \frac{1}{2}(p_y^2 + p_z^2) + \frac{\omega_x^2}{2}(y^2+z^2) + y^2z^2 \tag{6.1}$$

where again $\omega_x = \sqrt{2}x$ and x is assumed large. Deep in the channel, the final term can be thought of as a small perturbation which has virtually no effect on the eigenenergies. If that term were completely absent, the local Hamiltonian would have an $SU(2)$ symmetry corresponding to a two-dimensional harmonic oscillator. The eigenvalues of the Hamiltonian would then be $e_n = (n+1)\overline{h}\omega_x$, each with a degeneracy of $(n+1)$. The degenerate states can be labelled by the rotational quantum number m which runs from $-n$ to n in even increments. The perturbation y^2z^2 will not affect the energies in a significant manner but will act to break-up the degenerate collections of states into specific irreps of C_{4v} as follows. All states with odd m correspond to the E irrep. The $m = 0$ states are all A_1. For m non-zero and divisible by 4, the states are either A_1 or B_2 (corresponding to $\cos(m\theta)$ and $\sin(m\theta)$ respectively). Otherwise, if m is even but not divisible by 4, the states are either A_2 or B_1 (corresponding to $\sin(m\theta)$ and $\cos(m\theta)$ respectively.) We then define local heat kernels corresponding to the five irreps by adding the contributions of all values of n with the appropriate degeneracy factor for each irrep so that

$$\begin{aligned} z_{A_1}(\beta) &= \sum_{n=\text{even}} \left[\frac{n+4}{4}\right] \mathrm{e}^{-\beta\overline{h}\omega_x(n+1)} \\ z_{B_2}(\beta) &= \sum_{n=\text{even}} \left[\frac{n}{4}\right] \mathrm{e}^{-\beta\overline{h}\omega_x(n+1)} \\ z_{B_1}(\beta) &= z_{A_2}(\beta) = \sum_{n=\text{even}} \left[\frac{n+2}{4}\right] \mathrm{e}^{-\beta\overline{h}\omega_x(n+1)} \\ z_E(\beta) &= \sum_{n=\text{odd}} (n+1)\mathrm{e}^{-\beta\overline{h}\omega_x(n+1)} \end{aligned} \tag{6.2}$$

where $[x]$ is the largest integer less than or equal to x. Collectively these are

$$z_R(\beta) = \sum_{n=0}^{\infty} c_R(n)\mathrm{e}^{-\beta\overline{h}\omega_x(n+1)} \tag{6.3}$$

where $c_R(n)$ are degeneracy factors defined implicitly in (6.2).

To evaluate the traces, we integrate over the remaining x dependence

$$\begin{aligned} Z_R(\beta) &= \frac{1}{2\pi\overline{h}} \sum_n c_R(n) \int_{-\infty}^{\infty} \mathrm{d}p_x\, \mathrm{e}^{-\beta p_x^2/2} \int_Q^{\infty} \mathrm{d}x\, \mathrm{e}^{-\beta\overline{h}\sqrt{2}(n+1)x} \\ &\approx \sqrt{\frac{1}{4\pi\beta^3\overline{h}^4}} \sum_n c_R(n) \frac{\xi^{n+1}}{n+1} \end{aligned} \tag{6.4}$$

where we have defined $\xi = \exp(-\sqrt{2}\beta\overline{h}Q) \approx 1 - \sqrt{2}\beta\overline{h}Q$. (Note that this is different by a factor of 2 from the analogous variable in two-dimensions.) This discussion is in terms of the local irreps; what we really want, however, are the local class heat kernels. We can obtain these by appropriate combinations of the irreps as in (3.3) to arrive at the class sums

$$S(g;\beta) = \sum_n c(g,n) \frac{\xi^{n+1}}{n+1}. \tag{6.5}$$

For the moment we omit the prefactor of (6.4), this will be reintroduced later. The degeneracy factor $c(g,n)$ corresponding to a group element g is found by adding together the degeneracy factors $c_R(n)$ with the appropriate weightings as given by (3.2), i.e.

$$c(g,n) = \sum_R \eta_R(g) c_R(n). \tag{6.6}$$

We start with the identity element. As mentioned, a channel calculation is unnecessary, however, it is instructive to see that this is manifest in the calculation itself. Comparing (3.2) with (6.2) it is apparent that $c(I, n) = n + 1$ so that

$$\begin{aligned} S(I;\beta) = \sum_{n=0}^{\infty} \xi^{n+1} &= \frac{\xi}{1-\xi} \\ &\approx \frac{1}{\sqrt{2}\beta\overline{h}Q}. \end{aligned} \tag{6.7}$$

We now reinsert the prefactor of (6.4) and also an integral factor representing the number of channels left invariant by the corresponding element f_g, as in two-dimensions. We trivially have $f_I = 6$ so that the channel result for the identity element is

$$Z_c(I;\beta) \approx \frac{3}{\sqrt{2\pi}} \frac{1}{\beta^{5/2}\overline{h}^3 Q}. \tag{6.8}$$

Comparing this result to (5.5), the present contribution is very much smaller if $\beta^{1/4}Q \gg 1$ which is precisely the limit we are considering. Therefore, we confirm that no channel calculation is necessary for the identity element.

We next consider the reflection element σ_z. It is in the same class as σ_y so comparing (3.2) with (6.2) we conclude $c(\sigma_z, n) = 1$ when n is even and 0 when n is odd. The calculation which must be done is

$$\begin{aligned} S(\sigma_z;\beta) = \sum_{n=\text{even}} \frac{\xi^{n+1}}{n+1} &= \sum_{m=0}^{\infty} \frac{\xi^{2m+1}}{2m+1} \\ &\approx \frac{1}{2}\log\left(\frac{\sqrt{2}}{\beta\overline{h}Q}\right) \end{aligned} \tag{6.9}$$

where we have used (2.11) and the approximation immediately below (6.4). Note that $f_{\sigma_z} = 4$ since σ_z leaves four channels invariant, so that

$$Z_c(\sigma_z;\beta) \approx \sqrt{\frac{1}{\pi\beta^3\overline{h}^4}}\left(\log\frac{\sqrt{2}}{\beta\overline{h}} - \log Q\right). \tag{6.10}$$

Recalling now the corresponding result for the central region (5.7), we conclude that for the class C_3',

$$Z(C_3';\beta) \approx \sqrt{\frac{1}{16\pi\beta^3\overline{h}^4}}\left(\log\left(\frac{1}{\beta^3\overline{h}^4}\right) + \gamma + 4\log 2\right). \tag{6.11}$$

This is independent of Q as we expect.

The equality of z_{B_1} and z_{A_2} in (5.7) implies that $S(\sigma_3;\beta) = S(\sigma_z;\beta)$ (since they both equal $z_{A_1} - z_{B_2}$ from (3.2)). The only difference in the subsequent calculation is that $f_{\sigma_3} = 2$ so that the channel result for σ_3 is one half of that for σ_z (6.10). We combine this result with the result from the central region (5.9) to conclude

$$Z(C_5';\beta) \approx \sqrt{\frac{1}{64\pi\beta^3\overline{h}^4}}\left(\log\left(\frac{1}{\beta^3\overline{h}^4}\right) + \gamma + 8\log 2\right). \tag{6.12}$$

For rotations by $\pi/2$ about the x-axis we note that $c(R_{\pi/2}, n) = (-1)^{n/2}$ for n even and is 0 for n odd so that

$$\begin{aligned} S(R_{\pi/2};\beta) = \sum_{n=\text{even}} (-1)^{n/2} \frac{\xi^{n+1}}{n+1} &= \sum_{m=0}^{\infty} (-1)^m \frac{\xi^{2m+1}}{2m+1} \\ &= \arctan \xi \\ &\approx \frac{\pi}{4} - \frac{\beta\bar{h} Q}{\sqrt{2}} \end{aligned} \tag{6.13}$$

where we have again used (2.11). We now note that only two channels are left invariant implying $f_{R_{\pi/2}} = 2$ so that

$$Z_c(R_{\pi/2};\beta) \approx \sqrt{\frac{\pi}{16\beta^3\bar{h}^4}} - \sqrt{\frac{1}{2\pi\beta\bar{h}^2}}\, Q. \tag{6.14}$$

We now combine this with the calculation from the central region (5.10) to arrive at

$$Z(C_2;\beta) \approx \sqrt{\frac{\pi}{16\beta^3\bar{h}^4}}. \tag{6.15}$$

The final class is C_3 of which a rotation by π about the x-axis is a representative member. We then have $c(R_\pi, n) = (-1)^n$ so that the relevant calculation is

$$\begin{aligned} S(R_\pi;\beta) = \sum_{n=0}^{\infty} (-1)^n \xi^{n+1} &= \frac{\xi}{1+\xi} \\ &\approx \frac{1}{2}\left(1 - \frac{\beta\bar{h}}{\sqrt{2}} Q\right). \end{aligned} \tag{6.16}$$

We again have $f_{R_\pi} = 2$ so that the result of the channel calculation is

$$Z_c(R_\pi;\beta) \approx \sqrt{\frac{1}{4\pi\beta^3\bar{h}^4}} - \sqrt{\frac{1}{8\pi\beta\bar{h}^2}}\, Q. \tag{6.17}$$

Combining this with the calculation from the central region (5.11) we conclude

$$Z(C_3;\beta) \approx \sqrt{\frac{1}{4\pi\beta^3\bar{h}^4}}. \tag{6.18}$$

The final analysis we will do is to find the inverse Laplace transform of the various relations and thereby express them in the energy domain. The 10 results as a function of β are scattered over the previous two sections. As in the two-dimensions, we go directly to

the integrated densities of states by use of (2.14). The result is

$$\begin{aligned}
N(C_1;E) &\approx \frac{16\Gamma^2(\frac{1}{4})}{45\sqrt{2\pi^3}}y^3 \\
N(C_2;E) &\approx \tfrac{1}{3}y^2 \\
N(C_3;E) &\approx \frac{2}{3\pi}y^2 \\
N(C_4;E) &\approx \frac{\Gamma^2(\frac{1}{4})}{\sqrt{27\sqrt{3}\pi^3}}y \\
N(C_5;E) &\approx \frac{\Gamma^2(\frac{1}{4})}{6\sqrt{2\pi^3}}y \\
N(C_1';E) &\approx \tfrac{1}{8} \\
N(C_2';E) &\approx \tfrac{1}{4} \\
N(C_3';E) &\approx \frac{1}{3\pi}y^2(4\log y + 4\gamma + 10\log 2 - 8) \\
N(C_4';E) &\approx \tfrac{1}{6} \\
N(C_5';E) &\approx \frac{1}{6\pi}y^2(4\log y + 4\gamma + 14\log 2 - 8)
\end{aligned} \tag{6.19}$$

where again we use the semiclassically large quantity $y = E^{3/4}/\overline{h}$. For comparison, we remark that for generic potentials, use of (1.8), would imply that the first term scales as y^3, the following four as y, the set $\{C_1', C_2', C_4'\}$ as y^0, and the set $\{C_3', C_5'\}$ as y^2.

The leading-order behaviour, as given by the first expression, scales generically with $\overline{h}$. There are no other terms which are competitive with it so the relation that the fraction of states in irrep R is approximately $d_R^2/|G|$ and is valid. As mentioned, the reflection classes C_3' and C_5' are amplified somewhat, having a logarithmic dependence on $\overline{h}$ in addition to the $1/\overline{h}^2$ prefactor. This is in analogy to the total density of states of the two-dimensional problem. In fact, the class C_5' is, within a factor of four, the same as the total density of states in two-dimensions. Two of the rotation classes are amplified by $1/\overline{h}$ so that they scale as $1/\overline{h}^2$. This makes them competitive with the reflection classes (since, as argued in the two-dimensional problem, the logarithmic term is a rather weak amplification). This is analogous to the behaviour of one of the reflection operators in the two-dimensional case.

In figure 6 we show the integrated densities of states found from using the results of (6.19) combined according to the projection relation (2.16) and using the characters of table 5. It should be remarked that this may not be entirely consistent since the leading order terms might have semiclassical corrections which are of the same order or larger than the smallest terms we are considering. However, the point of this section is not a systematic semiclassical expansion but rather a study of the symmetry effects. The structure now looks more typical; irreps of the same-dimensionality have roughly similar numbers of states with slight differences arising from the contributions of the other group elements. In particular, the largest four curves are the four three dimensional irreps and the differences among them arise from the terms of order $y^2 \log y$ and y^2; the largest of these curves belongs to Γ_5'. The middle two curves belong to the two-dimensional irreps and the smallest four curves belong to the one-dimensional irreps. The largest of these is the trivial irrep Γ_1; this is reasonable since it receives positive contributions from all the classes.

In figure 7 we show the same data but on a smaller energy scale. At the right edge of the figure ($E = 35$), the curves are ordered the same as in figure 6 (i.e. their asymptotic

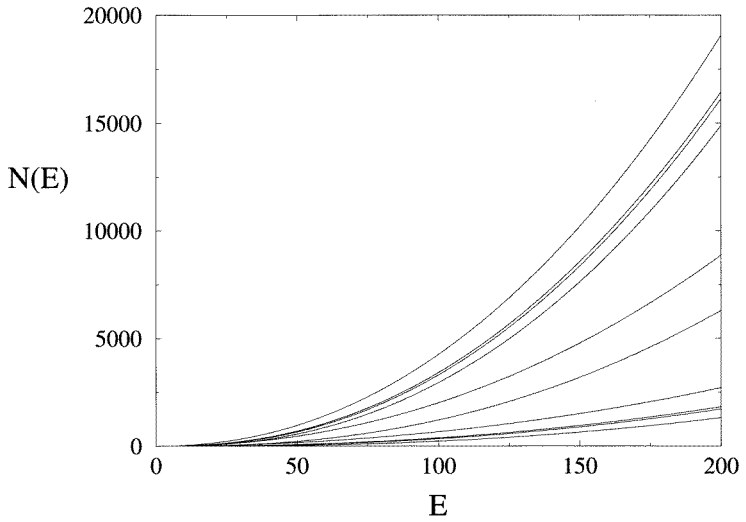

Figure 6. The average densities of states for each of the 10 irreps of the potential $V = x^2y^2 + y^2z^2 + z^2x^2$. From greatest to smallest the curves describe the irreps Γ_5', Γ_4, Γ_4', Γ_5, Γ_3, Γ_3', Γ_1, Γ_2', Γ_2 and Γ_1'.

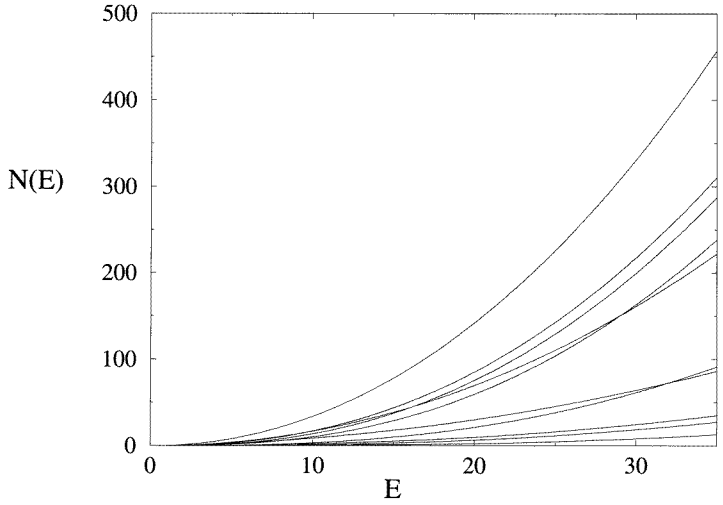

Figure 7. The same as figure 6 but on a smaller energy scale to show the curves crossing at small energies. At $E = 35$, the order of the curves is the same as that described in the previous figure caption.

ordering). However, it is clear that there is a lot of crossing of these curves at lower energies. This is because for moderate energies the contribution corresponding to identity in (6.19) does not dominate the others. Additionally, in calculating the functions for each irrep via (2.16) we must sum over all the group elements and so the contribution of any given class is amplified by the number of elements in that class. The identity class only has one element but the classes which contribute to next order, $\{C_2, C_3, C_3', C_5'\}$, have six, three, three and six elements respectively. As mentioned, it is difficult to calculate many accurate eigenvalues when a potential has channels and this is especially true in three-dimensions.

Therefore, the non-asymptotic behaviour in figure 7 is relevant to any numerical study since the results will probably all be in that energy domain.

7. Conclusion

We have shown that the symmetry reduction of the Thomas–Fermi density of states discussed in [17] is easily generalized to more perverse systems where direct use of the Wigner representation fails. In two-dimensions, the symmetry decomposition introduces essentially leading order contributions to the densities of states of the one-dimensional irreps. The results were verified numerically and seen to work well. However, the problem studied is numerically very difficult and only a handful of states of each irrep are reliably calculated. Nevertheless, certain combinations of the densities of states are found to be accurate to very high energies even though the density of states of each individual irrep is not. This effect is noticeable only by studying the class functions derived here and would not otherwise have been apparent, thus, underlining the importance of symmetry decompositions. We have also shown that the corrections in $\overline{h}$ are anomalously weak, being smaller than $\mathrm{O}(\overline{h})$.

In three-dimensions, we find that the symmetry decomposition does not introduce terms which are essentially leading order. However, there are still interesting effects; two of the reflection classes have a logarithmic dependence on $\overline{h}$ beyond what one might have expected and two of the rotation classes have an additional power of $1/\overline{h}$ thus making them of essentially the same order as the reflection elements. Furthermore, we observed that even in this case one must consider rather high energies before the ordering of the functions $N_R(E)$ achieves its final form. This is in spite of the fact that the leading behaviour is not affected by the decomposition. Rather it arises from the fact that the classes which contribute at next to leading order have several group elements and their contributions are correspondingly amplified. This is an effect which we can expect to become even more important in higher-dimensions if we consider potentials of the form $V(\{x_i\}) = \sum_i \sum_{j>i} x_i^2 x_j^2$. In higher-dimensions, more and more of the terms will behave with the normal $\overline{h}$ dependence. The only terms with anomalous dependences are those for which one would initially expect a dependence of $1/\overline{h}^2$ or $1/\overline{h}$. If the corresponding group element leaves at least one channel invariant, they will be amplified by factors of $\log(1/\overline{h})$ and $1/\overline{h}$ respectively.

Acknowledgments

I would like to thank Oriol Bohigas, Stephen Creagh, Per Dahlqvist, Dominique Delande, Gabriel Karl, Bent Lauritzen and Steve Tomsovic for useful discussions. I would also like to thank Dominique Delande for supplying numerical data used in checking the higher-order corrections. This work was supported by the Natural Sciences and Engineering Research Council of Canada.

References

[1] Müller B and Trayanov A 1992 *Phys. Rev. Lett.* **68** 3387
Gong C 1994 *Phys. Rev.* D **49** 2842
Biró T S *et al* 1994 *Int. J. Mod. Phys.* C **5** 13
Nielsen H B, Rugh H H and Rugh S E 1996 *Chaos and Scaling in Classical Non-Abelian Gauge Fields* chao-dyn/9605013
Muller B 1996 *Study of Chaos and Scaling in Classical SU(2) Gauge Theory* chao-dyn/9607001

[2] Matinyan S G, Savvidy G K and Ter-Arutyunyan-Savvidy N G 1981 *Sov. Phys. JEPT* **53** 421
Matinyan S G, Savvidy G K and Ter-Arutyunyan-Savvidy N G 1982 *JETP Lett.* **34** 590
Chirikov B V and Shepelyanskii D L 1981 *JETP Lett.* **34** 163
Savvidy G K 1984 *Nucl. Phys.* B **246** 302
Berman G, Bulgakov E, Holm D and Kluger Y 1994 *Phys. Lett.* A **194** 251
[3] Dahlqvist P and Russberg G 1990 *Phys. Rev. Lett.* **65** 2837
[4] Dahlqvist P 1992 *J. Phys. A: Math. Gen.* **25** 6265
[5] Dahlqvist P 1994 *J. Phys. A: Math. Gen.* **27** 763
[6] Tanner G and Wintgen D 1995 *Phys. Rev. Lett.* **75** 2928
[7] Tanner G, Hansen K T and Main J 1996 *Nonlinearity* **9** 1641
[8] Eckhardt B and Wintgen D 1990 *J. Phys. B: At. Mol. Opt. Phys.* **23** 355
[9] Zakrzewski J, Dupret K and Delande D 1995 *Phys. Rev. Lett.* **74** 522
[10] Martens C C, Waterland R L and Reinhardt W P 1989 *J. Chem. Phys.* **90** 2328
[11] Weiper F J *et al* 1996 *Phys. Rev. Lett.* **77** 2662
[12] Simon B 1983 *Ann. Phys.* **146** 209
[13] Tomsovic S 1991 *J. Phys. A: Math. Gen.* **24** L733
[14] Pavloff N 1994 *J. Phys. A: Math. Gen.* **27** 4317
[15] Bohigas O, Tomsovic S and Ullmo D 1993 *Phys. Rep.* **223** 43
[16] Sommermann H M and Weidenmüller H A 1993 *Europhys. Lett.* **23** 79
[17] Lauritzen B and Whelan N D 1995 *Ann. Phys* **244** 112
[18] Gutzwiller M C 1990 *Chaos in Classical and Quantum Mechanics* (New York: Springer)
[19] Hammermesh M 1962 *Group Theory and its Applications* (London: Addison-Wesley)
[20] Wigner E P 1932 *Phys. Rev.* **40** 749
[21] See, for example, Jennings B K, Bhaduri R K and Brack M 1975 *Nucl. Phys.* A **253** 28 and references therein.
[22] Grammaticos B and Voros A 1979 *Ann. Phys., NY* **123** 359
[23] Delande D Private communication
Gray C G *et al* to be published
[24] Steiner F and Trillenberg P 1990 *J. Math. Phys.* **31** 1670
[25] Robbins J 1989 *Phys. Rev.* A **40** 2128
[26] Tomsovic S Private communication.
[27] This analysis was greatly facilitated by data supplied to me by D Delande.
[28] Berry M V and Howls C J 1994 *Proc. R. Soc.* A **447** 527
[29] See, for example, Lomont J S 1959 *Applications of Finite Groups* (New York: Academic)